Title: ERK5 is required for neutrophil-mediated ROS release and essential in epidermolysis bullosa acquisita

Short Title: ERK5 in epidermolysis bullosa acquisita

Sören Dräger[1,2]*, Mareile Schlotfeldt[2]*, Leonie Voss[3], Sophia Johannisson[2,4], Michael Radziewitz[2], Colin Osterloh[2], Natalie Gross[2], Mayumi Kamaguchi[2], Ann-Kathrin Schneider[3], Gestur Vidarsson[5], Remco Visser[5], Frank Petersen[6], Xinhua Yu[6], Andreas Recke[1], Nancy Ernst[2], Anja Lux[3,7]*, and Katja Bieber[2]*

* *These authors contributed equally.*

Affiliations:

[1] *Department of Dermatology, Allergology and Venerology, University medical center Schleswig-Holstein (UKSH), Campus Lübeck, Germany*

[2] *Lübeck Institute of Experimental Dermatology and Center for Research on Inflammation of the Skin, University of Lübeck, Lübeck, Germany,*

[3] *Department of Biology, Institute of Genetics, Friedrich-Alexander University (FAU) Erlangen-Nürnberg, Erlangen, Germany*

[4] *Department of Dermatology, University of Heidelberg, Heidelberg, Germany*

[5] *Department of Biomolecular Mass Spectrometry and Proteomics, Utrecht Institute for Pharmaceutical Sciences and Bijvoet Center for Biomolecular Research, Utrecht University, Utrecht, The Netherlands*

[6] *Priority Area Asthma and Allergy, Research Center Borstel, Airway Research Center North, German Center for Lung Research, Borstel, Germany,*

[7] *Profile Centre Immunomedicine, Friedrich-Alexander University (FAU), Erlangen, Germany*

Corresponding author:

Sören Dräger, MD; University medical center Schleswig-Holstein, Department of Dermatology, Allergology and Venerology, Ratzeburger Allee 160, 23562 Lübeck; +49 451 500 41550

soeren.draeger@uksh.de

https://orcid.org/0000-0002-3701-8365

The authors have declared that no conflict of interest exists.

Keywords: antibody-mediated autoimmune diseases, pemphigoid diseases, rheumatoid arthritis, neutrophils, autoimmunity

Word count: 4926

Figures: 4

Supplemental: Figures: 1

Tables: 0

Abstract (max 200 words)

Neutrophils are key effector cells in antibody-mediated autoimmune diseases, contributing to inflammation via the release of reactive oxygen species (ROS). Extracellular signal-regulated kinase 5 (ERK5), a member of the MAPK family, is expressed in neutrophils but its role in autoimmune disease pathogenesis remains unclear. We investigated the functional relevance of ERK5 in antibody-mediated autoimmune diseases by comparing neutrophil-dependent (epidermolysis bullosa acquisita, EBA; serum transfer arthritis, STA) and neutrophil-independent (immune thrombocytopenia, ITP) murine models using the small-molecule ERK5 inhibitor XMD8-92. *In vitro*, pharmacological ERK5 inhibition specifically reduced neutrophil ROS release and CD62L shedding without affecting adhesion, chemotaxis, or CD18 expression. No major effects on viability were observed. *In vivo*, ERK5 inhibition with XMD8-92 significantly ameliorated antibody transfer-induced EBA, supporting a critical role of neutrophil-derived ROS in disease pathogenesis. In STA and ITP, ERK5 inhibition did not affect clinical outcomes. Together, these findings highlight ERK5 as a regulator of neutrophil ROS release and a potential therapeutic target in ROS-driven autoimmune diseases such as EBA.

Introduction:

Neutrophils are the most abundant granulocytes and key effector cells of the innate immune system (1). They are recruited from the circulation to the site of inflammation through a multi-step process (2), including selectins, chemoattractants and integrins and - in the context of autoimmune diseases – are activated by deposited antibodies/immune complexes (ICs) via Fc gamma receptors (FcγR) (3). In the context of antibody-mediated diseases, e.g. autoimmune blistering disorders such as pemphigoid diseases, human neutrophils are activated via FcγRIIA and FcγRIIIB (3). Correspondingly in mice, FcγRIV is critical for pathogenesis (4), whereas FcγRIIB is inhibitory (5). FcγR activation by IgG leads to internal signal transduction via spleen tyrosine kinase (SYK), transforming growth factor-β-activated kinase 1 (TAK1) and the mitogen activated protein kinase (MAPK)/mitogen-activated protein kinase kinase (MEK)/extracellular signal-regulated kinases (ERK) signaling cascade (1). Consequently, inhibiting these pathways can alleviate disease, which has been shown for example for SYK (6) or PI3K (7–9) in murine models of epidermolysis bullosa acquisita (EBA). Notably, a recent high-throughput screening of a drug library identified several repurposable drugs targeting polymorphonuclear leukocytes (PMNs) (10). Since neutrophils contribute to the inflammation with their effector functions, such as the release of reactive oxygen species (ROS) (11,12) and proteases, such as neutrophil elastase (13) or granzyme B (14), this opens possibilities for further treatment exploration.

As ERK5 is expressed in neutrophils (15) and upregulated upon activation (7), it represents a promising target for therapeutic intervention in diseases primarily driven by neutrophils. ERK5, encoded by the *MAPK7* gene and also known as big MAP-kinase 1 (BMK1), is a member of the MAPK family, which are serine/threonine kinases centrally involved in a range of cellular processes including proliferation, differentiation, migration, responses to stress, cell survival and regulation of inflammation (16). Whereas the classical MAPK pathways including ERK1/2, p38, and JNK pathways are already extensively characterized in neutrophil immune responses and autoimmune diseases (17–19), the function of ERK5 in this context is largely unknown. However, in other cell types such as endothelial cells and monocytes, ERK5 is associated with e.g. oxidative stress (20), inflammation (21) and survival signaling (22). Since these processes also play a role in activated neutrophils (23), we hypothesize that ERK5 is involved in immune complex-induced

kinase signaling in neutrophils. It acts downstream of MAP kinase kinase kinase (MEKK2/3) and MAPK2 MEK5, and is engaged by a variety of stimuli, e.g. cytokines, hormones, mitogens and stress-factors like shear stress and high osmolarity (24). In its closed inactive conformation, ERK5 is complexed with heat shock protein 90 (HSP90) and the co-chaperone cell division cycle 37 (CDC37), exposing a nuclear export signal (25,26). Upon phosphorylation by MEK5, cyclin dependent kinase (CDK) 5, CDK1 or ERK1, ERK5 auto-phosphorylates several residues within its C-terminal extension, resulting in conformational changes, dissociation from HSP90 and exposure of the formerly hidden nuclear localization signal (27). After transport into the nucleus, ERK5 mediates phosphorylation of MEF2 transcription factors and also acts as a transcription factor itself (28,29). The pathophysiological role of ERK5 in disease has been extensively reviewed elsewhere (24,30). ERK5 has primarily been investigated in cancer, such as hematological malignancies and melanoma, where ERK5 inhibition induced senescence of melanoma cells (31). However, its role in autoimmune disorders is underexplored, with only few published studies on this topic. For example, in psoriasiform dermatitis, treatment with the ERK5 inhibitor AX-15836 reduced disease severity and inhibited neutrophil extracellular trap (NET) formation (32). ERK5 is also required for B cell activating factor (BAFF)-induced B cell survival (33), hence, inhibition of ERK5 might be beneficial in antibody-mediated autoimmune diseases.

Based on the aforementioned data and the prominent role of neutrophils in the effector phase of antibody mediated diseases, we designed this study to clarify the role of ERK5 in antibody-mediated autoimmune diseases by contrasting neutrophil-dependent and -independent conditions. To highlight pathogenic differences and to assess the impact of ERK5, we selected three murine models representing prototypical antibody-mediated autoimmune diseases. EBA and serum transfer arthritis (STA) (as a model for rheumatoid arthritis (RA)) were chosen as examples of neutrophil-driven diseases. Due to distinct involved autoantigens, EBA is characterized by dermal-epidermal separation leading to skin blistering (34) and STA by swelling of joints accompanied by bone and cartilage destruction(35). The pathogenesis of both diseases has been shown to be highly neutrophil-dependent (11,12,36) but in contrast to EBA, an additional role for macrophages, mast cells, and NKT cells has been shown in STA (35). To further delineate a possible neutrophil-specific effect, the impact of ERK5 inhibition in immune thrombocytopenia (ITP) was

evaluated, a disease model considered neutrophil-independent (37). Here, platelet-bound IgG autoantibodies induce immune cell signaling mainly through FcγRI and FcγRIV (37), resulting in the subsequent phagocytosis and destruction of platelets in reticuloendothelial organs driven by tissue-resident macrophages (37–42).

The use of murine disease models has been invaluable in advancing our understanding of the disease pathogenesis and in uncovering potential therapeutic strategies (6,7,34,43,44). Aiming to uncover the role of ERK5 in IgG-driven autoimmunity, we herein investigate the impact of pharmacological ERK5 inhibition in antibody-mediated neutrophil-dependent (EBA and RA) and neutrophil-independent (ITP) autoimmune disease models.

Materials and Methods

Animal experimentation

C57BL/6J mice (Charles River, Germany) were bred in a specific pathogen–free environment and provided standard mouse chow and acidified drinking water *ad libitum*. Mice of both sexes, aged 8 to 14 weeks, were used for experimental models, with clinical examinations, biopsies, and bleeding procedures performed under anesthesia, either using isoflurane or intraperitoneal (i.p.) administration of a ketamine (75 mg/kg, Sigma-Aldrich, Taufkirchen, Germany) and medetomidine (1 mg/kg, Vetoquinol, Ismaning, Germany) mixture antagonised after ca. 30 min by atipamezole (5 mg/kg, Vetoquinol). On the final day, the mice were euthanized either using 15 mg/kg xylazine (Sigma-Aldrich) and 100 mg/kg ketamine and cervical dislocation or carbon dioxide.

Sampling of human biomaterials

For the isolation of human neutrophils, whole blood was drawn from healthy volunteers after informed consent was given. All experiments using human samples were approved by the local ethics committee (AZ #20-463, University of Lübeck, Lübeck, Germany) and were performed in accordance with the Declaration of Helsinki.

Chemicals

All standard chemicals were supplied by Carl Roth (Karlsruhe, Germany) or Sigma-Aldrich (Taufkirchen, Germany). XMD8-92 was supplied by Selleckchem (Cologne, Germany) (Cambridge, UK). For *in vitro* assays, 10 mM XMD8-92 was dissolved in DMSO and further diluted to final concentrations of 1 µM, 0.1 µM, 0.01 µM and 10 µM. For *in vivo* experiments, XMD8-92 was dissolved in 30 % hydroxypropyl β-cyclodextrin, which also served as the vehicle control.

Immunohistochemical staining of phosphorylated ERK5 (pERK5)

Paraffin-embedded skin specimens from control and immunization-induced EBA mice (45) or STA were used for immunohistochemical staining of pErk5. Immunohistochemistry was performed as previously described with modifications (46). Deparaffinization and rehydration were performed using standard protocols followed by heat-induced antigen retrieval in citrate buffer at pH 6 for 10 min at

310 °C. Samples were washed in tris-buffered saline (TBS) and permeabilized with 0.5 % (v/v) Triton X-100 in 6 % (w/v) bovine serum albumin (BSA) in TBS for 30 min at room temperature (RT). Blocking was performed with 10 % (v/v) normal goat serum in TBS for 30 min at 37 °C. Incubation with the primary antibody (anti-pErk5, PA5-114573, Invitrogen, Waltham, USA) diluted 1:200 in 2 % normal goat serum in TBS was performed for 1.5 h at RT. Subsequently, slides were incubated for 1 h at RT with goat anti-rabbit IgG H&L AP (ab97048, abcam) diluted 1:500 in 2 % normal goat serum in TBS. SIGMAFAST™ Fast Red (Sigma-Aldrich) served as substrate. Nuclei were counterstained with hematoxylin. Stained sections were evaluated by light microscopy (Keyence BZ-9000E, Osaka, Japan). Analysis was performed in a blinded, semi-quantitative manner, separately for the dermis and the epidermis. Expression was evaluated by visual inspection with scores of 0 (no staining), 1 (> 0 %, but ≤ 10 % positive cells), 2 (> 10 %, but ≤ 50 % positive cells), and 3 (> 50 % positive cells).

Secretion of complement component C5a by HaCaTs

Immortalized keratinocyte (HaCaT) cells (47) were cultured with the cell culture medium Keratinocyte Growth Medium 2 (KGM2; Bio&Sell, Feucht, Germany) supplemented with Supplement Mix (PromoCell GmbH, Heidelberg, Germany), 0.06 mM $CaCl_2$ (PromoCell GmbH, Heidelberg, Germany) and grown to confluency on 48-well plates at 5 x 10^4 cells/well. After culturing for 18 h, HaCaT cells were pre-incubated with XMD8-92 at concentrations of 10 µM, 1 µM, 100 nM, 10 nM, or 1 nM (in 0.1 % DMSO) for 5 min followed by stimulation with affinity purified anti-COL7-IgG from EBA patients (80 µg/mL), as previously described.(7,48) Cells stimulated with anti-COL7-IgG in absence of XMD8-92 (with 0.1 % DMSO) served as a positive control. Cells stimulated with human IVIG (Intratect, Biotest Pharma GmbH, Dreieich, Germany) in the presence of 10 µM of XMD8-92 served as negative control. Cells were incubated for 24 h, after which supernatants were removed and stored at -20 °C. C5a concentration in supernatants was determined using the Human Complement Component C5a DuoSet ELISA (R&D Systems GmbH, Wiesbaden, Germany) in accordance with manufacturer instructions and measured in a GloMax® Discover microplate reader (Promega, Walldorf, Germany).

Human PMN purification

For ROS release assay, flow cytometry, and adhesion assay, PMNs were isolated from EDTA-treated human whole blood performing a PolymorphPrep™ (Serumwerk Bernburg AG, Bernburg, Germany) density gradient centrifugation as previously described (49). For the chemotaxis assay, PMNs were purified from citrated human whole blood using a Ficoll gradient (50). Blood was diluted 1:2 with 1 % (w/v) polyvinyl alcohol and allowed to sediment for 25 min. The supernatant was cautiously added to Ficoll-Paque™ PLUS (Cytiva, Marlborough, USA) and centrifuged for 24 min at 850 g without brake. Erythrocyte lysis was performed on the pellet using distilled water and stopped with 2x phosphate-buffered saline (PBS). After washing, the cells were diluted to 4×10^5 cells/mL in 1 % (w/v) BSA in PBS. Neutrophil purity was assessed in flow cytometry for all experiments and was higher than 85 % for all samples.

ROS release assay

Plates were coated with ICs consisting of human COL7 E-F at 2.5 µg/mL and anti-human COL7 IgG1 at 1.8 µg/mL as previously described (51,52). PMNs (2×10^5 cells/well) were added in the presence or absence of XMD8-92. Only antibody (with cells), only antigen (with cells), or only cells served as negative controls, while PMA (10 nM/mL) served as a positive control. DMSO was adjusted to a final concentration of 0.01 %. All samples were measured in duplicates. Luminol was added to each well to reach a final concentration of 90 µg/mL and luminescence was measured every 2 min for 2 h at 37 °C using a GloMax® Discover microplate reader (Promega, Walldorf, Germany). The area under the curve (AUC) was calculated and values were normalized to IC-stimulated cells without XMD8-92.

Adhesion assay

PMN adhesion was assessed using impedance-based real-time cell analysis as described previously (53). Briefly, a 96-well E-plate (Agilent, Santa Clara, USA) was coated with ICs as described for the ROS release assay. Inhibitor solutions were prepared and added to the plate before transferring PMNs (2×10^5 cells/well). Impedance was measured every 2 min for 120 min using in an xCELLigence system (Agilent, Santa Clara, USA) and expressed as the cell index in arbitrary units. Data were analyzed as described for the ROS release assay.

Chemotaxis assay

The chemotactic capacity of neutrophils was assessed using 48-well Boyden chambers (NeuroProbe Inc., Gaithersburg, USA) as described before(49,54). Human PMNs were isolated as previously stated. The lower chamber was blocked with 1 % (w/v) BSA in 0.1 M Na_2CO_3/0.1 M $NaHCO_3$ (pH 9) for 1 h at 37 °C in a humid chamber. After buffer removal, 5 nM IL-8 (Peprotech, Hamburg, Germany) was loaded to the lower chamber and covered with a polycarbonate membrane (pore size 3 µm; Costar Nucleopore GmbH, Tübingen, Germany). The fully assembled chamber was incubated for 30 min at 37 °C. The PMN suspension was brought to a final concentration of 0.9 mM $CaCl_2$ and 0.5 mM $MgCl_2$ and pre-warmed in a water bath at 37 °C. XMD8-92 was added at the respective concentrations. The cell-inhibitor suspension was added to the upper chamber. Following incubation (1 h at 37 °C), myeloperoxidase assay was performed on the migrated cells. For this, the cells from the lower chamber were transferred to a microplate and lysed with an equal volume of 0.2 % hexadecyltrimethylammonium bromide. In parallel, a standard of lysed cells was applied to determine the cell number. TMB substrate (Promega) was added to the wells for approximately 2 min before stopping the reaction with 1 M H_2SO_4. Absorbance was read at 450 nm in a GloMax® Discover microplate reader (Promega, Walldorf, Germany).

Flow cytometry

Human PMNs were isolated as previously described and stimulated with ICs, prepared in the same manner as for the ROS release assay, for 2 h at 37 °C in a 5 % CO□ atmosphere. Subsequently, they were stained for the flow cytometric analysis of the following surface markers using standard flow cytometry procedures: CD14 (clone HCD14), CD16 (clone 3G8), CD18 (clone 1B4/CD18), CD45 (clone HI30), and CD62L (clone DREG-56), CD193 (clone 5E8). Viability was assessed by Annexin V (B266195) and Zombie NIR staining (B308933).(49) All dyes were purchased from BioLegend (San Diego, USA). Measurements were performed on a MACSQuant® Analyzer 10 (Miltenyi Biotec, Bergisch Gladbach, Germany) and analysis was conducted using MACS Quantify (version 2.13.3, Miltenyi Biotec).

Local antibody-transfer induced experimental EBA

Specific anti–mouse COL7^{C} IgG from rabbit serum was isolated as described previously (55–57). XMD8-92 was administered p.o. twice daily at 50 mg/kg body weight, beginning one day before the anti–mouse COL7^{C} IgG injection and was performed daily throughout the 5-day experiment. C57BL/6J mice of both sexes, aged 11-14 weeks, were injected in the base of the ear once with 100 µg rabbit anti–mouse COL7^{C} IgG. Mice were evaluated clinically every day, and the percentage of the affected ear surface area and ear thickness were assessed using a Mitutoyo 7301 dial thickness gauge (Neuss, Germany) by person unaware of the treatment. Ears were collected on the final day of the local antibody-transfer induced experimental EBA, cut in half and embedded in 4 % PBS-buffered paraffin or frozen in liquid nitrogen. Paraffin-embedded samples were subjected to hematoxylin-eosin staining. Split formation, cell infiltration, and epidermal thickness were evaluated as described before (46). Frozen samples were used for direct immunofluorescence staining detecting IgG and C3 deposits as described previously (56).

Serum-transfer arthritis (STA)

Serum transfer arthritis (STA) was induced by injection of arthritogenic KBxN serum in 8 week old female C57BL/6J mice at 10 µL/g bodyweight as described before (58). Before and after arthritis induction, mice were treated twice daily with 50 mg/kg body weight XMD8-92 or vehicle control p.o. Severity of joint swelling was evaluated over the course of seven days by scoring the swelling of individual paws on a scale of 0-3. Scores were added for a total clinical score. Peripheral blood was collected retro-orbitally on day 0 and day 7 and inflammatory cytokines were quantified in the serum by LegendPlex multiplex assay (Mouse Inflammation 13-plex, BioLegend) as a parameter of systemic inflammation. On day 7, mice were sacrificed, and forelegs were prepared for histological analysis. Hematoxylin & eosin staining was performed to evaluate inflammatory infiltrates and Safranin-O staining to assess bone and cartilage damage, respectively, as previously described (59,60). At the end of the *in vivo* arthritis experiments, both front paws of the mice were prepared and skin and surrounding muscle tissue were roughly removed. The paws were incubated overnight in 4 % PFA at 4 °C for fixation. Subsequently, bones were decalcified with Immunocal™ (Immunotec, Los Angeles, USA) for six days. For Safranin-O staining, nuclei were stained with Weigert solution (Weigert's hematoxylin solution A and B 1:2, Carl Roth) for 3 min and washed in running water for 15 min. Sections were

incubated in Scott's buffer (1 % $MgSO_4$, 0.2 % $NaHCO_3$ in ddH_2O), followed by water for 2 min each. Green color was achieved by incubation in Goldner solution III (Carl Roth), immersion in 1 % acetic acid and incubation in water for 30 s. Proteoglycans were stained with 0.1 % Safranin-O (Carl Roth) for 5 min. Sections were immersed in water, incubated for 1 min in 100 % ethanol and 3 min in xylol. Stained sections were evaluated by light microscopy using a Zeiss Axiovert 200 microscope and the AxioVision LE4.6 software (Olympus Life Science, Waltham, USA).

Immune thrombocytopenia (ITP)

Platelet depletion in presence of kinase inhibition was assessed in 8 week old female C57BL/6J mice, as previously described (41). Platelet depletion was induced by injection of 0.35 µg/g anti-platelet IgG2c (clone 6A6) upon treatment with vehicle control or XMD8-92 (50 mg/kg body weight applied p.o.) 24 h and 4 h before the induction of platelet depletion. Platelet counts in peripheral blood were assessed before 6A6-IgG2c injection, and at 4 h and 24 h post-injection in peripheral blood collected retro-orbitally. Platelet counts were determined using an ADVIA® 2120i hematocytometer (Siemens Healthineers, Germany).

Statistical analysis

Data were analyzed using Prism 10.4.1 (GraphPad Software, San Diego, USA). Statistical tests were performed as indicated. $p \leq 0.05$ was considered significant. (*$p \leq 0.05$; **$p \leq 0.01$; ***$p \leq 0.001$; ****$p \leq 0.0001$).

Study approval

Animal experiments were approved by local authorities of the Animal Care and Use Committee (*Government of Schleswig-Holstein* and government of Lower Franconia) and performed by certified personnel (AZ 108/08-15 and *55.2.2-2532-2-2085*) following the ARRIVE guidelines.

Data availability

The data that support the findings of this study are available from the corresponding author upon reasonable request.

Results

ERK5 inhibition selectively reduces ROS release from immune-complex–stimulated neutrophils

Neutrophil activation and recruitment to the inflamed tissue is a complex multistep process (61). To assess the role of ERK5 in various neutrophil effector functions, we conducted several *in vitro* assays focusing on the following characteristics: ROS release, expression of the surface activation markers CD18 and CD62L, adhesion, and chemotaxis. Furthermore, potential toxic effects on neutrophils were investigated. In each assay, four different concentrations of the ERK5 inhibitor XMD8-92 (10 µM, 1 µM, 0.1 µM, and 0.01 µM) were used. While we could not show any differences in either the surface expression of CD18, adhesion, nor chemotaxis, ROS release was significantly reduced by the ERK5 inhibitor in a dose-dependent manner, with an IC_{50} of 1.469 µM. In addition, less CD62L shedding was observed at 10 µM and 0.01 µM. Of note, viability was slightly lower at 10 µM. However, since less than 1 % of the cells were affected, the biological significance is probably negligible (Figure 1 A-F).

ERK5 is activated in lesional skin of EBA mice, and its inhibition by XMD8-92 alleviates disease development without affecting keratinocyte C5a release or antibody deposition

Kinases are crucially involved in the signaling of a variety of cellular responses in health and disease, including autoimmune diseases (62). Therefore, we hypothesized that ERK5 is critically involved in the pathogenesis of EBA, which is a neutrophil-driven autoimmune skin disease (63). To investigate this, we measured the phosphorylated and thus active ERK5 (pERK5) in skin samples obtained from the immunization-induced EBA mouse model. pErk5 was subjected to immunohistochemistry targeting the residues T219 and Y221. These residues are known to be involved in the activation of ERK5 (64). Protein expression in epidermis and dermis was quantified separately. We could indeed observe enhanced staining of pERK5 in lesional skin compared to healthy skin in epidermis and dermis(Figure 2A,B).

The presence of pERK5 in keratinocytes indicates the necessity of further investigation into the role of ERK5 in keratinocyte function since keratinocytes play a

crucial role in attracting neutrophils to the skin by releasing inflammatory mediators such as C5a upon activation (57,65). To evaluate the impact of ERK5 inhibition on C5a production, we again used the small-molecule inhibitor XMD8-92. The immortalized human keratinocyte cell line HaCaT was used to determine C5a levels by ELISA following stimulation with purified anti-COL7-IgG from EBA patients. No significant changes in C5a secretion were observed (Figure 2C). Therefore, C5a production by keratinocytes appears to be independent of ERK5.

Since the inhibition of ERK5 significantly reduced ROS release, a major hallmark of EBA pathogenesis (66), we proceeded to evaluate XMD8-92's inhibitory potential *in vivo*. XMD8-92 was administered in a prophylactic approach to assess its impact on disease development and progression of the antibody transfer-induced EBA model. Dose and treatment schedule were adapted from a previous publication using XMD8-92 (67). Briefly, C57BL/6J mice were injected with rabbit anti-mouse COL7^{c}-IgG (7,49), and treated orally twice daily with XMD8-92 or vehicle, starting one day before disease induction, and subsequently, disease was scored daily (Figure 2D).
Clinical disease score and increase in ear thickness were significantly reduced at all time points (Figure 2E, F). On day 3, affected ear surface area (AESA) measured 48.3 % in the vehicle group compared to 25.0 % in the treatment group. Ear thickness amounted to 250 µm in the vehicle group, compared to 83 µm in the treatment group. Histological examination revealed that leukocyte infiltration was unaffected by ERK5 inhibition (Figure 3G). Split formation showed a tendency to be reduced, however, this did not reach statistical significance ($p = 0.12$) (Figure 2 H). As anticipated, IgG and C3 deposition showed no significant differences between the groups (Figure 2I, J).

ERK5 inhibition does not alter STA disease severity

Given that the development of EBA, a neutrophil-dependent disease, was affected by ERK5 inhibition, we hypothesized that targeting ERK5 could similarly prove effective in other neutrophil-driven autoimmune diseases, such as RA. A commonly used model for RA is STA (35), which was employed here. In contrast to EBA, mast cells, monocytes, macrophages and osteoclasts are also thought to play a major role in STA pathogenesis (59). By an immunohistological staining of pERK5, we could demonstrate an increased expression of pERK5 in inflammatory infiltrates found in

the legs of STA mice compared to healthy controls. (Figure 3A). Thus, we investigated whether ERK5 inhibition by XMD8-92 could improve the pathological phenotype similar to EBA. Therefore, STA was induced in C57BL/6J mice by injection of serum derived from arthritic KBxN mice. Joint swelling was monitored for 7 days and blood was sampled at day 0 and 7 to assess cytokine levels as an indicator of systemic inflammation (Figure 3B). No significant difference was observed between the two groups regarding the arthritis score (Figure 3C) but a significantly higher serum concentration of IFN-γ was identified, showing a four-fold increase in the treatment group compared to the control group after 7 days (Figure 3D). However, several other cytokines remained unchanged (Supplemental Figure 1). Histological stainings were performed to assess leukocyte infiltration (H&E) and cartilage damage (Safranin-O), and findings correlated with the varying clinical disease scores within treatment and vehicle group (Figure 3E).

ERK5 inhibition does not affect platelet depletion in passive ITP model

To complement the *in vivo* analyses and gain insight into neutrophil specificity of ERK5 inhibition, XMD8-92 was tested in a non-neutrophil-dependent autoimmune disease model, specifically ITP. Similar to RA/STA and EBA, ITP is an autoantibody-mediated disease that can be accurately modelled experimentally, however, different cell types such as macrophages are involved in the effector phase. Platelet depletion was induced in C57BL/6J mice by i.p. injection of platelet-specific IgG2c. Platelet counts were measured prior to depletion and at 4 h and 24 h post-injection (Figure 4A). As expected, ERK5 inhibition did neither affect platelet depletion nor recovery (Figure 4B).

Discussion

Since current treatments for autoimmune diseases rely on general, untargeted immunosuppression with a low safety profile failing to induce remission in all patients (68), identifying additional therapeutic targets remains essential. In this study, we investigated the functional role of ERK5 in three prototypical autoantibody-mediated diseases, contrasting neutrophil-dependent and -independent ones. Neutrophils, as components of the innate immune system, function as key effector cells in many autoimmune diseases (11). They cause tissue inflammation and damage by performing a variety of cellular functions, including adhesion, chemotaxis, cytokine release, NET formation, ROS production, and phagocytosis (1) . To broadly characterize neutrophils *in vitro*, we assessed, surface activation marker expression (CD18 and CD62L), adhesion, chemotaxis, and ROS release. ERK5 inhibition by XMD8-92 specifically reduced CD62L shedding and ROS release, without notably impacting viability. Although viability was significantly lower at the highest concentration tested, the percentage of viable cells was still in the range of the negative controls, and thus probably not of biological relevance. Likewise, CD18 expression, chemotaxis and adhesion were not affected, suggesting that later steps in neutrophil activation are affected. The ability of substances to inhibit ROS release *in vitro* indicates their potential to ameliorate ROS-dependent diseases *in vivo*, as demonstrated in both, the immunization-induced and the antibody transfer-induced EBA mouse models in recent studies (6,7,10,49).

Activation of the ERK5 signaling pathway during neutrophil-dependent inflammation is *suggested* by the increased expression of pERK5, as observed in EBA-affected skin. In contrast, pharmacological ERK5 inhibition did not influence C5a secretion by HaCaT cells upon stimulation with anti-COL7-IgG.

In the antibody transfer-induced EBA mouse model, the systemic application of ERK5 inhibitor XMD8-92 alleviated disease progression from day 1 onwards. The degree of disease improvement was comparable to that achieved with treatments such as propranolol (49). As expected, the deposition of IgG and complement component C3 remained unchanged. Furthermore, leukocyte infiltration was unaltered which is in line with the unchanged chemotaxis observed *in vitro.* Split formation, primarily driven by ROS release, showed a tendency to be reduced; however, this difference did not reach statistical significance.

To assess the impact of ERK5 inhibition across antibody-mediated neutrophil-dependent and -independent diseases, two additional murine models were included alongside EBA: STA and ITP. In the EBA model, as in KBxN-STA, neutrophils are the main cell type found in inflamed tissue. ITP on the other hand is completely independent of neutrophils, with macrophages being the main driver of pathogenesis (40,69). As only antibody-transfer-induced EBA was ameliorated, it is important to emphasize the distinct pathogenic mechanisms underlying these disease models. Accordingly, the observed disease-specific efficacy of XMD8-92 suggests that the inhibitor indeed preferentially targets neutrophils and not cells of the mononuclear-phagocytic network. Alternatively, a major difference between passive EBA and STA to be considered is the activation of distinct signaling pathways, possibly leading to different effector mechanisms. In addition to neutrophils, macrophages and osteoclasts also contribute to STA pathogenesis. Furthermore, FcγRIII and FcγRIV signalling mediates inflammation in STA (35), while tissue damage in EBA is mainly mediated via FcγRIV(4) .

The hallmark of EBA is the release of reactive oxygen species (ROS). Here, neutrophil cytosolic factor 1 (Ncf1)-deficient mice, which cannot generate ROS through NADPH oxidase, are completely protected from disease manifestation (66). Opposingly, as defects in nitrogen or ROS production could not rescue mice from developing arthritis, it has been hypothesized that NET formation and cytokine release might be more important for pathogenesis than ROS production (36). Moreover, Ncf1-deficient mice showed increased arthritis severity, which was partly attributed to the accumulation of neutrophils in the joints, along with upregulated pro-inflammatory characteristics (70). Interestingly, the source of ROS appears to be important, as macrophage-derived ROS can suppress T cell activation in an Ncf-1 dependent manner (71).

With cytokine production being a relevant factor for STA pathogenesis, systemic cytokine levels were measured before disease onset and at the peak of arthritis development. Albeit minor increases in IL-6 and IL-27 could be observed over the course of the disease, low overall concentrations of inflammatory cytokines in serum of STA mice are in line with the model primarily involving joint inflammation. Nevertheless, XMD8-92 treatment was associated with increased serum IFN-γ levels. Produced by Th1, $CD8^+$ T cells and NK cells, IFN-γ appears to exhibit immunomodulatory functions in RA patients treated with anti-TNF treatment

adalimumab (72). In murine models of antigen-induced arthritis, IFN-γ deficiency has accordingly been associated with more severe disease (73). While this supports a potentially disease-modifying role of XMD8-92 in arthritis, no significant clinical differences in disease progression were observed herein. The reasons behind this remain speculative and require further research.

In ITP on the other hand, interventions targeting the production of platelets, specifically megakaryocytes, or the effector cells in the reticuloendothelial organs (40,69), would most likely lead to a reduction of the disease severity. Our data show that inhibition of ERK5 is negligible for this process. Interestingly, platelets themselves also express ERK5 (74). Further investigation is necessitated, as other members of the ERK family have been implicated in regulating megakaryocyte differentiation (75,76).

A limitation of our study is the exclusive use of an inhibitory compound rather than a targeted deletion of *Erk5*. Furthermore, XMD8-92 functions as a dual inhibitor, targeting both bromodomains (BRDs) and ERK5 (77). BRDs are conserved structural modules found in chromatin- and transcription-associated proteins, where they play a role in epigenetic regulation and transcriptional regulation by recognizing acetylated histones (78–80). The effects of XMD8-92 may, in part, be due to its ability to inhibit BRD4. Therefore, further studies should be conducted using more selective ERK5 inhibitors to better isolate its specific effects (77). Studying ERK5's isolated effects is challenging, as its substrates, the MEF2 transcription factors, can regulate myeloid cell fate by regulating the balance between monopoiesis and granulopoiesis (81). Furthermore, we focused specifically on neutrophils but cannot exclude effects on other ERK5-expressing cells.

In our study, functional analysis of neutrophils revealed a specific role for ERK5 in ROS release, while other neutrophil functions following IC stimulation remained unaffected. Supporting the existing notion that the capacity to inhibit ROS release predicts *in vivo* efficacy, inhibition of ERK5 by XMD8-92 significantly reduced disease severity in the antibody transfer-induced EBA model. Contrarily, in STA and ITP ERK5 appears dispensable. These findings suggest that ERK5 plays a critical role in EBA pathogenesis, particularly in the effector phase by modulating ROS release from neutrophils.

References

1. Zhang F, Xia Y, Su J, Quan F, Zhou H, Li Q, et al. Neutrophil diversity and function in health and disease. Signal Transduct Target Ther. 2024 Dec 6;9(1):343.

2. Springer TA. Traffic signals for lymphocyte recirculation and leukocyte emigration: The multistep paradigm. Cell. 1994 Jan;76(2):301–14.

3. Ludwig RJ, Vanhoorelbeke K, Leypoldt F, Kaya Z, Bieber K, McLachlan SM, et al. Mechanisms of autoantibody-induced pathology. Front Immunol. 2017;8.

4. Kasperkiewicz M, Nimmerjahn F, Wende S, Hirose M, Iwata H, Jonkman MF, et al. Genetic identification and functional validation of FcγRIV as key molecule in autoantibody-induced tissue injury. J Pathol. 2012 Sept;228(1):8–19.

5. Karsten CM, Pandey MK, Figge J, Kilchenstein R, Taylor PR, Rosas M, et al. Anti-inflammatory activity of IgG1 mediated by Fc galactosylation and association of FcγRIIB and dectin-1. Nat Med. 2012;18(9):1401–6.

6. Samavedam UK, Mitschker N, Kasprick A, Bieber K, Schmidt E, Laskay T, et al. Whole-genome expression profiling in skin reveals SYK As a key regulator of inflammation in experimental epidermolysis bullosa acquisita. Front Immunol. 2018;9(FEB).

7. Zillikens H, Kasprick A, Osterloh C, Gross N, Radziewitz M, Hass C, et al. Topical Application of the PI3Kβ-Selective Small Molecule Inhibitor TGX-221 Is an Effective Treatment Option for Experimental Epidermolysis Bullosa Acquisita. Front Med. 2021 Sept 7;8:713312.

8. Ghorbanalipoor S, Emtenani S, Parker M, Kamaguchi M, Osterloh C, Pigors M, et al. Cutaneous kinase activity correlates with treatment outcomes following PI3K delta inhibition in mice with experimental pemphigoid diseases. Front Immunol. 2022 Sept 28;13:865241.

9. Koga H, Kasprick A, López R, Aulí M, Pont M, Godessart N, et al. Therapeutic effect of a novel phosphatidylinositol-3-Kinase δ inhibitor in experimental epidermolysis bullosa acquisita. Front Immunol. 2018;9(JUL):1–12.

10. Ghorbanalipoor S, Matsumoto K, Gross N, Heimberg L, Krause M, Veldkamp W, et al. High throughput screening identifies repurposable drugs for modulation of innate and acquired immune responses. J Autoimmun. 2024 Sept;148:103302.

11. Shimanovich I, Mihai S, Oostingh GJ, Ilenchuk TT, Bröcker EB, Opdenakker G, et al. Granulocyte-derived elastase and gelatinase B are required for dermal-epidermal separation induced by autoantibodies from patients with epidermolysis bullosa acquisita and bullous pemphigoid. J Pathol. 2004;204(5):519–27.

12. Chiriac M, Roesler J, Sindrilaru A, Scharffetter-Kochanek K, Zillikens D, Sitaru C. NADPH oxidase is required for neutrophil-dependent autoantibody-induced tissue damage. J Pathol. 2007;212(March):56–65.

13. Liu Z, Shapiro SD, Zhou X, Twining SS, Senior RM, Giudice GJ, et al. A critical role for neutrophil elastase in experimental bullous pemphigoid. J Clin Invest. 2000;105(1):113–23.

14. Emtenani S, Lebhar H, Marquis CP, Ludwig RJ, Schmidt E. Granzyme B inhibition reduces autoantibody-induced dermal–epidermal separation in an ex vivo model of epidermolysis bullosa acquisita. Exp Dermatol. 2024 Sept;33(9):e15172.

15. Hii CS, Anson DS, Costabile M, Mukaro V, Dunning K, Ferrante A. Characterization of the MEK5-ERK5 Module in Human Neutrophils and Its Relationship to ERK1/ERK2 in the Chemotactic Response. J Biol Chem. 2004 Nov;279(48):49825–34.

16. Cargnello M, Roux PP. Activation and Function of the MAPKs and Their Substrates, the MAPK-Activated Protein Kinases. Microbiol Mol Biol Rev. 2011 Mar;75(1):50–83.

17. Müller S, Behnen M, Bieber K, Möller S, Hellberg L, Witte M, et al. Dimethylfumarate Impairs Neutrophil Functions. J Invest Dermatol. 2016 Jan;136(1):117–26.

18. Vorobjeva NV. Involvement of Mitogen-Activated Protein Kinases p38 and ERK1/2, as well as Protein Kinase B Akt1/2, in the Formation of Neutrophil Extracellular Traps. Mosc Univ Biol Sci Bull. 2023 Dec;78(4):219–24.

19. Zarrin AA, Bao K, Lupardus P, Vucic D. Kinase inhibition in autoimmunity and inflammation. Nat Rev Drug Discov. 2021 Jan;20(1):39–63.

20. Tusa I, Menconi A, Tubita A, Rovida E. Pathophysiological Impact of the MEK5/ERK5 Pathway in Oxidative Stress. Cells. 2023 Apr 13;12(8):1154.

21. Wilhelmsen K, Xu F, Farrar K, Tran A, Khakpour S, Sundar S, et al. Extracellular signal–regulated kinase 5 promotes acute cellular and systemic inflammation. Sci Signal [Internet]. 2015 Aug 25 [cited 2025 Oct 28];8(391). Available from: https://www.science.org/doi/10.1126/scisignal.aaa3206

22. Gírio A, Montero JC, Pandiella A, Chatterjee S. Erk5 is activated and acts as a survival factor in mitosis. Cell Signal. 2007 Sept;19(9):1964–72.

23. Aroca-Crevillén A, Vicanolo T, Ovadia S, Hidalgo A. Neutrophils in Physiology and Pathology. Annu Rev Pathol Mech Dis. 2024 Jan 24;19(1):227–59.

24. Le NT. The significance of ERK5 catalytic-independent functions in disease pathways. Front Cell Dev Biol. 2023 Aug 4;11:1235217.

25. Kondoh K, Terasawa K, Morimoto H, Nishida E. Regulation of Nuclear Translocation of Extracellular Signal-Regulated Kinase 5 by Active Nuclear Import and Export Mechanisms. Mol Cell Biol. 2006 Mar 1;26(5):1679–90.

26. Erazo T, Moreno A, Ruiz-Babot G, Rodríguez-Asiain A, Morrice NA, Espadamala J, et al. Canonical and Kinase Activity-Independent Mechanisms for Extracellular Signal-Regulated Kinase 5 (ERK5) Nuclear Translocation Require Dissociation of Hsp90 from the ERK5-Cdc37 Complex. Mol Cell Biol. 2013 Apr 1;33(8):1671–86.

27. Gomez N, Erazo T, Lizcano JM. ERK5 and Cell Proliferation: Nuclear Localization Is What Matters. Front Cell Dev Biol. 2016 Sept 22;4.

28. Morimoto H, Kondoh K, Nishimoto S, Terasawa K, Nishida E. Activation of a C-terminal Transcriptional Activation Domain of ERK5 by Autophosphorylation. J Biol Chem. 2007 Dec;282(49):35449–56.

29. Kasler HG, Victoria J, Duramad O, Winoto A. ERK5 Is a Novel Type of Mitogen-Activated Protein Kinase Containing a Transcriptional Activation Domain. Mol Cell Biol. 2000 Nov 1;20(22):8382–9.

30. Paudel R, Fusi L, Schmidt M. The mek5/erk5 pathway in health and disease. Int J Mol Sci. 2021;22(14).

31. Tubita A, Lombardi Z, Tusa I, Lazzeretti A, Sgrignani G, Papini D, et al. Inhibition of ERK5 Elicits Cellular Senescence in Melanoma via the Cyclin-Dependent Kinase Inhibitor p21. Cancer Res. 2022 Feb 1;82(3):447–57.

32. Ding Y, Ouyang Z, Zhang C, Zhu Y, Xu Q, Sun H, et al. Tyrosine phosphatase SHP2 exacerbates psoriasis-like skin inflammation in mice via ERK5-dependent NETosis. MedComm. 2022 Mar;3(1):e120.

33. Jacque E, Schweighoffer E, Tybulewicz VLJ, Ley SC. BAFF activation of the ERK5 MAP kinase pathway regulates B cell survival. J Exp Med. 2015 June 1;212(6):883–92.

34. Tigges M, Dräger S, Piccini I, Bieber K, Vorobyev A, Edelkamp J, et al. Pemphigoid disease model systems for clinical translation. Front Immunol. 2025 Mar 17;16:1537428.

35. Christensen AD, Haase C, Cook AD, Hamilton JA. K/BxN Serum-Transfer Arthritis as a Model for Human Inflammatory Arthritis. Front Immunol. 2016 June 2;7.

36. Wipke BT, Allen PM. Essential Role of Neutrophils in the Initiation and Progression of a Murine Model of Rheumatoid Arthritis. J Immunol. 2001 Aug 1;167(3):1601–8.

37. Biburger M, Aschermann S, Schwab I, Lux A, Albert H, Danzer H, et al. Monocyte Subsets Responsible for Immunoglobulin G-Dependent Effector Functions In Vivo. Immunity. 2011 Dec;35(6):932–44.

38. Semple JW. Animal models of immune thrombocytopenia (ITP). Ann Hematol. 2010 July;89(S1):37–44.

39. Zufferey A, Kapur R, Semple J. Pathogenesis and Therapeutic Mechanisms in Immune Thrombocytopenia (ITP). J Clin Med. 2017 Feb 9;6(2):16.

40. Norris PAA, Tawhidi Z, Sachs UJ, Cserti-Gazdewich CM, Lin Y, Callum J, et al. Serum from half of patients with immune thrombocytopenia triggers macrophage phagocytosis of platelets. Blood Adv. 2023 July 25;7(14):3561–72.

41. Wöhner M, Brechtelsbauer S, Friedrich N, Vorsatz C, Bulang J, Liang C, et al. Tissue niche occupancy determines the contribution of fetal- versus bone-

marrow-derived macrophages to IgG effector functions. Cell Rep. 2024 Feb;43(2):113757.

42. Nimmerjahn F, Bruhns P, Horiuchi K, Ravetch JV. FcγRIV: A Novel FcR with Distinct IgG Subclass Specificity. Immunity. 2005 July;23(1):41–51.

43. Dräger S, Kalies K, Sidronio TB, Witte M, Ludwig RJ, Bieber K. Increased TREM-1 expression in inflamed skin has no functional impact on the pathogenesis of cutaneous disorders. J Dermatol Sci. 2017 May 29;88:139–55.

44. Bieber K, Sun S, Ishii N, Kasperkiewicz M, Schmidt E, Hirose M, et al. Animal models for autoimmune bullous dermatoses. Exp Dermatol. 2010 Jan;19(1):2–11.

45. Kasprick A, Bieber K, Ludwig RJ. Drug Discovery for Pemphigoid Diseases. Curr Protoc Pharmacol. 2019 Mar;84(1):e55.

46. Gross N, Marketon J, Mousavi S, Kalies K, Ludwig RJ, Bieber K. Inhibition of interferon gamma impairs induction of experimental epidermolysis bullosa acquisita. Front Immunol. 2024;15:1343299.

47. Boukamp P, Petrussevska RT, Breitkreutz D, Hornung J, Markham A, Fusenig NE. Normal keratinization in a spontaneously immortalized aneuploid human keratinocyte cell line. J Cell Biol. 1988 Mar 1;106(3):761–71.

48. Vorobyev A, Ujiie H, Recke A, Buijsrogge JJA, Jonkman MF, Pas HH, et al. Autoantibodies to Multiple Epitopes on the Non-Collagenous-1 Domain of Type VII Collagen Induce Blisters. J Invest Dermatol. 2015 June;135(6):1565–73.

49. Stüssel P, Schulze Dieckhoff K, Künzel S, Hartmann V, Gupta Y, Kaiser G, et al. Propranolol Is an Effective Topical and Systemic Treatment Option for Experimental Epidermolysis Bullosa Acquisita. J Invest Dermatol. 2020 Dec;140(12):2408–20.

50. Skoog WA, Beck WS. Studies on the Fibrinogen, Dextran and Phytohemagglutinin Methods of Isolating Leukocytes. Blood. 1956 May 1;11(5):436–54.

51. Recke A, Trog LM, Pas HH, Vorobyev A, Abadpour A, Jonkman MF, et al. Recombinant Human IgA1 and IgA2 Autoantibodies to Type VII Collagen Induce Subepidermal Blistering Ex Vivo. J Immunol. 2014 Aug 15;193(4):1600–8.

52. Yu X, Holdorf K, Kasper B, Zillikens D, Ludwig RJ, Petersen F. FcγRIIA and FcγRIIIB Are Required for Autoantibody-Induced Tissue Damage in Experimental Human Models of Bullous Pemphigoid. J Invest Dermatol. 2010 Dec;130(12):2841–4.

53. Yu X, Akbarzadeh R, Pieper M, Scholzen T, Gehrig S, Schultz C, et al. Neutrophil Adhesion Is a Prerequisite for Antibody-Mediated Proteolytic Tissue Damage in Experimental Models of Epidermolysis Bullosa Acquisita. J Invest Dermatol. 2018 Sept;138(9):1990–8.

54. Boyden S. The chemotactic effect of mixtures of antibody and antigen on polymorphonuclear leucocytes. J Exp Med. 1962 Mar 1;115(3):453–66.

55. Bieber K, Ernst AL, Tukaj S, Holtsche MM, Schmidt E, Zillikens D, et al. Analysis of serum markers of cellular immune activation in patients with bullous pemphigoid. Exp Dermatol. 2017 Dec;26(12):1248–52.

56. Bieber K, Witte M, Sun S, Hundt JE, Kalies K, Dräger S, et al. T cells mediate autoantibody-induced cutaneous inflammation and blistering in epidermolysis bullosa acquisita. Sci Rep. 2016 Dec 5;6(1):38357.

57. Sitaru C, Mihai S, Otto C, Chiriac MT, Hausser I, Dotterweich B, et al. Induction of dermal-epidermal separation in mice by passive transfer of antibodies specific to type VII collagen. J Clin Invest. 2005 Apr 1;115(4):870–8.

58. Seeling M, Pöhnl M, Kara S, Horstmann N, Riemer C, Wöhner M, et al. Immunoglobulin G-dependent inhibition of inflammatory bone remodeling requires pattern recognition receptor Dectin-1. Immunity. 2023 May;56(5):1046-1063.e7.

59. Seeling M, Hillenhoff U, David JP, Schett G, Tuckermann J, Lux A, et al. Inflammatory monocytes and Fcγ receptor IV on osteoclasts are critical for bone destruction during inflammatory arthritis in mice. Proc Natl Acad Sci. 2013 June 25;110(26):10729–34.

60. Seeling M, Pöhnl M, Kara S, Horstmann N, Riemer C, Wöhner M, et al. Immunoglobulin G-dependent inhibition of inflammatory bone remodeling requires pattern recognition receptor Dectin-1. Immunity. 2023 May;56(5):1046-1063.e7.

61. Kolaczkowska E, Kubes P. Neutrophil recruitment and function in health and inflammation. Nat Rev Immunol. 2013 Mar;13(3):159–75.

62. Zarrin AA, Bao K, Lupardus P, Vucic D. Kinase inhibition in autoimmunity and inflammation. Nat Rev Drug Discov. 2021 Jan;20(1):39–63.

63. Koga H, Prost-Squarcioni C, Iwata H, Jonkman MF, Ludwig RJ, Bieber K. Epidermolysis Bullosa Acquisita: The 2019 Update. Front Med [Internet]. 2019;5(January). Available from: https://www.frontiersin.org/article/10.3389/fmed.2018.00362/full

64. Mody N, Campbell DG, Morrice N, Peggie M, Cohen P. An analysis of the phosphorylation and activation of extracellular-signal-regulated protein kinase 5 (ERK5) by mitogen-activated protein kinase kinase 5 (MKK5) in vitro. Biochem J. 2003 June 1;372(2):567–75.

65. Sadik CD, Miyabe Y, Sezin T, Luster AD. The critical role of C5a as an initiator of neutrophil-mediated autoimmune inflammation of the joint and skin. Semin Immunol. 2018 June;37:21–9.

66. Chiriac MT, Roesler J, Sindrilaru A, Scharffetter-Kochanek K, Zillikens D, Sitaru C. NADPH oxidase is required for neutrophil-dependent autoantibody-induced tissue damage. J Pathol. 2007;212(1):56–65.

67. Yang Q, Deng X, Lu B, Cameron M, Fearns C, Patricelli MP, et al. Pharmacological Inhibition of BMK1 Suppresses Tumor Growth through Promyelocytic Leukemia Protein. Cancer Cell. 2010 Sept;18(3):258–67.

68. Lamberts A, Euverman HI, Terra JB, Jonkman MF, Horváth B. Effectiveness and safety of rituximab in recalcitrant pemphigoid diseases. Front Immunol. 2018;9(FEB):1–9.

69. Krémer V, de Chaisemartin L, Jönsson F. The role of neutrophils in antibody-driven autoimmune cytopenias. Int J Biochem Cell Biol. 2022 June 1;147:106231.

70. Liao YC, Wu SY, Huang YF, Lo PC, Chan TY, Chen CA, et al. NOX2-Deficient Neutrophils Facilitate Joint Inflammation Through Higher Pro-Inflammatory and Weakened Immune Checkpoint Activities. Front Immunol. 2021 Sept 7;12:743030.

71. Gelderman KA, Hultqvist M, Pizzolla A, Zhao M, Nandakumar KS, Mattsson R, et al. Macrophages suppress T cell responses and arthritis development in mice by producing reactive oxygen species. J Clin Invest. 2007 Oct 1;117(10):3020–8.

72. Aravena O, Pesce B, Soto L, Orrego N, Sabugo F, Wurmann P, et al. Anti-TNF therapy in patients with rheumatoid arthritis decreases Th1 and Th17 cell populations and expands IFN-γ-producing NK cell and regulatory T cell subsets. Immunobiology. 2011 Dec;216(12):1256–63.

73. Irmler IM, Gajda M, Bräuer R. Exacerbation of Antigen-Induced Arthritis in IFN-γ-Deficient Mice As a Result of Unrestricted IL-17 Response. J Immunol. 2007 Nov 1;179(9):6228–36.

74. Cameron SJ, Ture SK, Mickelsen D, Chakrabarti E, Modjeski KL, McNitt S, et al. Platelet Extracellular Regulated Protein Kinase 5 Is a Redox Switch and Triggers Maladaptive Platelet Responses and Myocardial Infarct Expansion. Circulation. 2015 July 7;132(1):47–58.

75. Séverin S, Ghevaert C, Mazharian A. The mitogen-activated protein kinase signaling pathways: role in megakaryocyte differentiation. J Thromb Haemost. 2010 Jan;8(1):17–26.

76. Mazharian A, Watson SP, Séverin S. Critical role for ERK1/2 in bone marrow and fetal liver–derived primary megakaryocyte differentiation, motility, and proplatelet formation. Exp Hematol. 2009 Oct;37(10):1238-1249.e5.

77. Lin ECK, Amantea CM, Nomanbhoy TK, Weissig H, Ishiyama J, Hu Y, et al. ERK5 kinase activity is dispensable for cellular immune response and proliferation. Proc Natl Acad Sci. 2016 Oct 18;113(42):11865–70.

78. Cochran AG, Conery AR, Sims RJ. Bromodomains: a new target class for drug development. Nat Rev Drug Discov. 2019 Aug;18(8):609–28.

79. Mann MW, Fu Y, Gearhart RL, Xu X, Roberts DS, Li Y, et al. Bromodomain-containing Protein 4 regulates innate inflammation via modulation of alternative splicing. Front Immunol. 2023 June 26;14:1212770.

80. Wang N, Wu R, Tang D, Kang R. The BET family in immunity and disease. Signal Transduct Target Ther. 2021 Jan 19;6(1):23.

81. Schüler A, Schwieger M, Engelmann A, Weber K, Horn S, Müller U, et al. The MADS transcription factor Mef2c is a pivotal modulator of myeloid cell fate. Blood. 2008 May 1;111(9):4532–41.

Figure legends

Figure 1.

ERK5 inhibition selectively reduces ROS release and CD62L shedding from immune-complex (IC)–stimulated polymorphonuclear leukocytes (PMNs).

Different cellular functions of neutrophil granulocytes were measured using increasing concentrations of the ERK5 inhibitor XMD8-92 (10 µM, 1 µM, 0.1 µM, 0.01 µM). **(A)** IC-induced ROS release was measured using a luminol-based assay, showing a dose-dependent reduction (IC_{50} = 1.469 µM). **(B)** PMN adhesion upon IC-stimulation was investigated using impedance-based measurements, which revealed no significant changes. **(C)** Boyden chamber chemotaxis to IL-8 was measured using the myeloperoxidase assay. Chemotaxis was not altered by ERK5 inhibition. Surface expression of the cell activation markers, measured by flow cytometry of **(D)** CD18 and **(E)** CD62L shedding was reduced at 0.01 µM and 10 µM. **(F)** Cell viability, determined by staining for Annexin V and Zombie NIR, was slightly affected at 10 µM. All results were normalized to the respective controls without the ERK5 inhibitor. n = 5. Values are displayed as mean ± SEM. A nonlinear fit dose response curve was calculated. Kruskal-Wallis test with Dunn's multiple comparisons test. *$p \leq 0.05$.

Figure 2.

ERK5 is activated in lesional skin of Epidermolysis bullosa acquisita (EBA) *ex vivo*, and its inhibition by XMD8-92 alleviates disease development *in vivo* without affecting keratinocyte C5a release or antibody deposition *in vitro*.

(A) Lesional and healthy skin obtained from immunization-induced EBA and healthy control mice was immunohistochemically stained for phosphorylated ERK5 (pERK5). Scale bar represents 100 µM. The dermal-epidermal junction is indicated by the black lines. Arrows indicate stained cells. **(B)** Enhanced staining in both dermis and epidermis in lesional treated mice was observed in a semi-quantitative measurement. **(C)** Immortalized keratinocytes (HaCaT) were stimulated with anti-$COL7^C$ IgG and C5a concentration was measured using ELISA, which showed no significant changes upon ERK5 inhibition. **(D-F)** Antibody transfer–induced EBA was induced by injection of rabbit anti-$mCOL7^C$ antibodies in C57BL/6J mice, and prophylactic treatment with XMD8-92 twice daily significantly reduced clinical disease scores, affected ear surface area (AESA), and delta ear thickness (referring to day 0) compared to vehicle

control. **(G,H)** In skin samples obtained on the final day of the antibody transfer–induced EBA model**,** histological analyses revealed no significant effects of ERK5 inhibition on leukocyte infiltration (asterisk) or dermal–epidermal split formation (arrows). IgG or C3 deposition remained unchanged (arrows).

(I–J) Cryosections were stained for IgG and C3 deposition, which were both unaffected by ERK5 inhibition.

B: n = 5, Tukey boxplot Mann-Whitney test, *p ≤ 0.05; **C**: n = 3, , mean ± SEM ; **E**: n = 6 (control)/5 (XMD8-92), mean ± SEM, mixed effect analysis with Šidák's multiple comparisons test, **p ≤ 0.01, ***p ≤0.001, ****p ≤ 0.0001; **G-J**: n = 6 (control)/5 (XMD8-92), Tukey boxplot, Mann-Whitney test

Figure 3.

ERK5 inhibition does not affect serum-transfer arthritis (**STA) severity**

(A) Schematic overview of STA, which was induced in female C57BL/6J mice by injection of arthritogenic KBxN serum. Mice were treated with XMD8-92 twice daily. **(B)** Clinical arthritis scores were comparable between vehicle- and XMD8-92–treated groups over 7 days. **(C)** Serum samples were collected at day 0 and 7 and cytokine analysis revealed significant higher IFN-γ concentrations in XMD8-92–treated mice on day 7. Paws were collected on the final day of the experiment and **(D)** Immunohistochemistry demonstrated dense infiltrates of pERK5-positive cells in affected joints (asterisk) **(E)** Histological staining (H&E for leukocyte infiltration (arrows); Safranin-O for cartilage damage (asterisk)) reflected clinical disease scores.

B: n = 4 (control)/5 (XMD8-92), mean ± SEM, n.s., mixed effect analysis with Šidák's multiple comparisons test; **C**: n = 4, Tukey box plot, 2-way ANOVA, *p ≤ 0.05

Figure 4.

Treatment with XMD8-92 does not influence platelet depletion or recovery in immune thrombocytopenia (ITP).

(A) ITP was induced in female C57BL/6J mice by i.p injection of anti-platelet IgG2c and platelet counts were measured at baseline and 4 and 24 h post-injection. **(B)** Absolute platelet count and **(C)** relative platelet count to baseline was comparable between XMD8-92- and vehicle-treated mice.

B, C: n = 5 (control)/4 (XMD8-92), mean ± SEM, mixed effect analysis with Šidák's multiple comparisons test.

Supplemental Figure 1:

Most cytokine concentrations in serum samples collected at day 0 and 7 of serum transfer arthritis (STA) are unaffected by treatment with XMD8-92.

STA was induced by i.p. injection of arthritic KBxN serum. On day 0 and 7, serum samples were taken from STA and control mice. Cytokine levels were measured using a LegendPlex™ multiplex assay. n = 4, Tukey box plot, 2-way ANOVA.

CReDit author contributions:

SD - Investigation, Formal analysis, Writing – Original draft

MS - Investigation, Formal analysis, Writing – Original draft

LV - Investigation, Formal analysis

SJ - Investigation, Formal analysis

MR - Investigation, Formal analysis

CO - Investigation, Formal analysis

NG - Investigation, Formal analysis

MK - Investigation, Formal analysis

AS – Investigation, Formal analysis

GV - Methodology, Supervision

RV - Methodology, Supervision

FP - Methodology, Supervision

XY - Methodology, Supervision

AR - Methodology, Supervision

NE - Methodology, Supervision

AL- Conceptualization, Resources, Methodology, Funding acquisition, Supervision

KB - Conceptualization, Resources, Methodology, Funding acquisition, Supervision

All authors reviewed and edited the manuscript.

Acknowledgments:

We thank Claudia Kauderer, Astrid Fischer and Alexandra Wobig for excellent technical assistance.

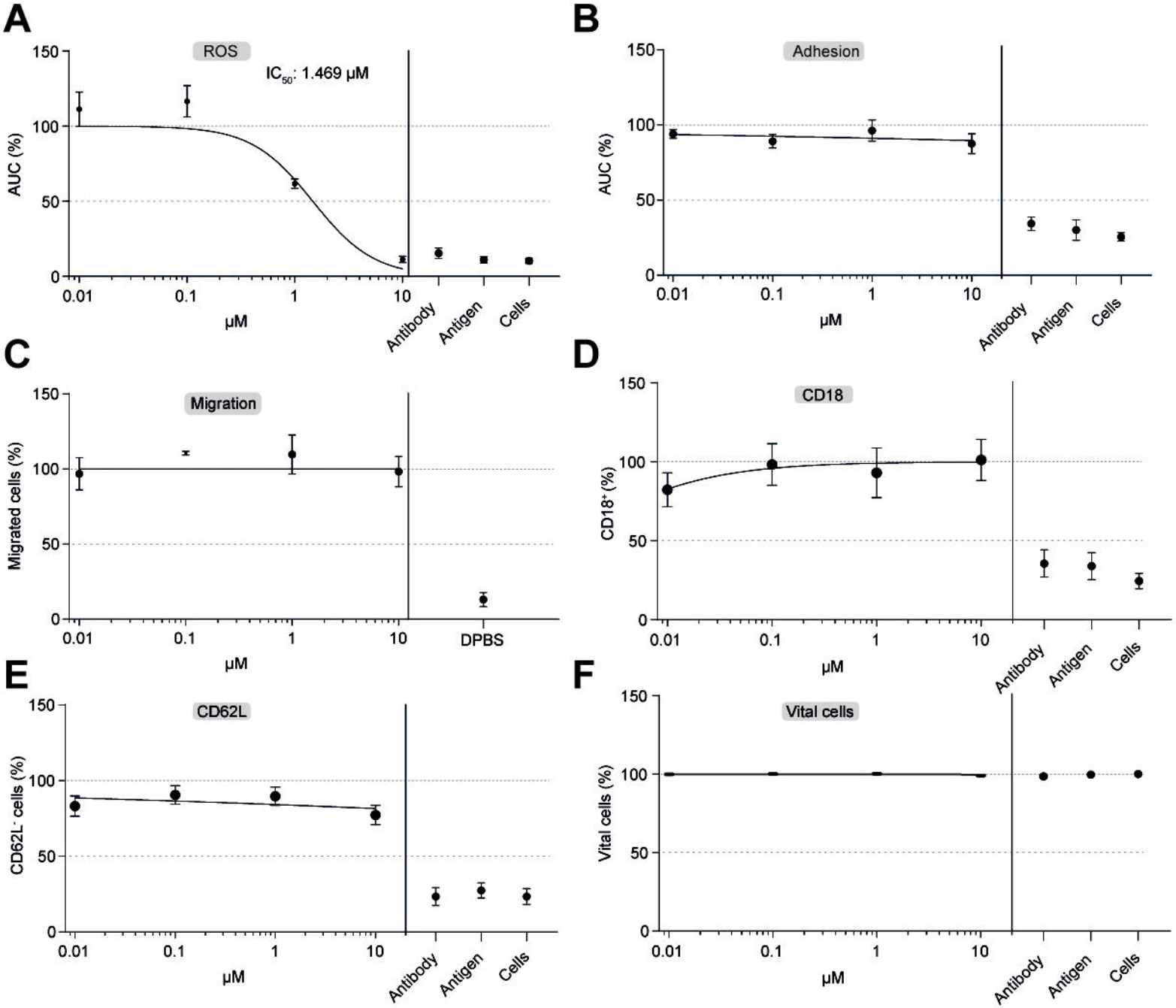
A
ROS
IC50: 1.469 µM
AUC (%)
µM
Antibody
Antigen
Cells
B
Adhesion
AUC (%)
µM
Antibody
Antigen
Cells
C
Migration
Migrated cells (%)
µM
DPBS
D
CD18
CD18+ (%)
µM
Antibody
Antigen
Cells
E
CD62L
CD62L- cells (%)
µM
Antibody
Antigen
Cells
F
Vital cells
Vital cells (%)
µM
Antibody
Antigen
Cells

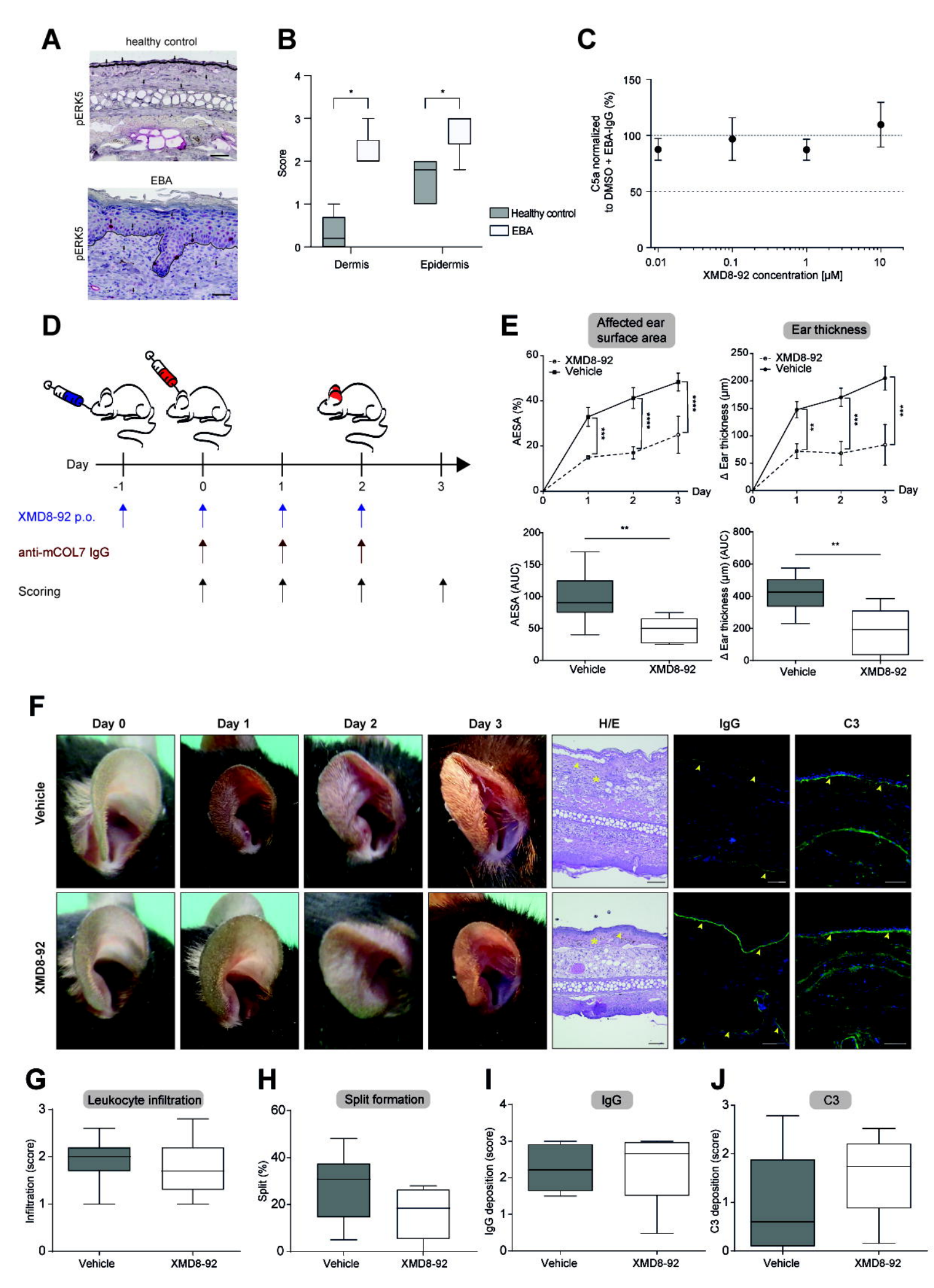
A
healthy control
pERK5
EBA
pERK5
B
Score
Dermis
Epidermis
Healthy control
EBA
C
C5a normalized to DMSO + EBA-IgG (%)
XMD8-92 concentration [µM]
D
Day
XMD8-92 p.o.
anti-mCOL7 IgG
Scoring
E
Affected ear surface area
Ear thickness
XMD8-92
Vehicle
AESA (%)
Δ Ear thickness (µm)
AESA (AUC)
Δ Ear thickness (µm) (AUC)
F
Day 0
Day 1
Day 2
Day 3
H/E
IgG
C3
Vehicle
XMD8-92
G
Leukocyte infiltration
Infiltration (score)
H
Split formation
Split (%)
I
IgG
IgG deposition (score)
J
C3
C3 deposition (score)

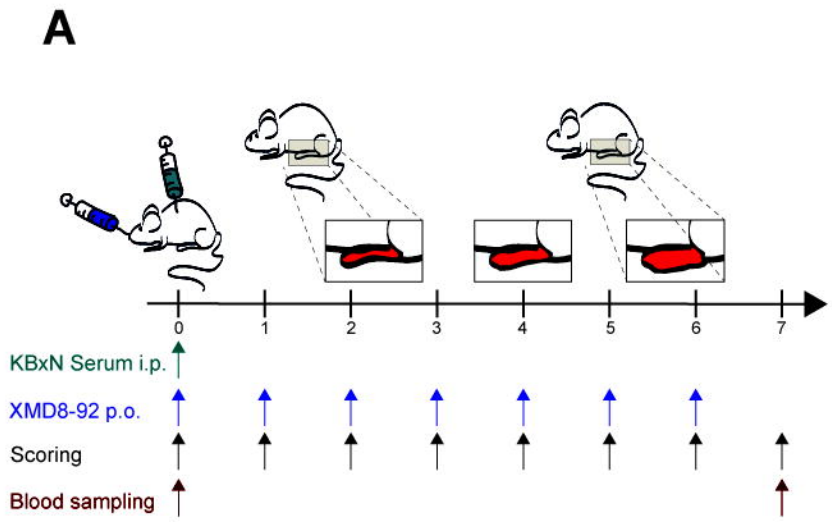
A
0
1
2
3
4
5
6
7
KBxN Serum i.p.
XMD8-92 p.o.
Scoring
Blood sampling

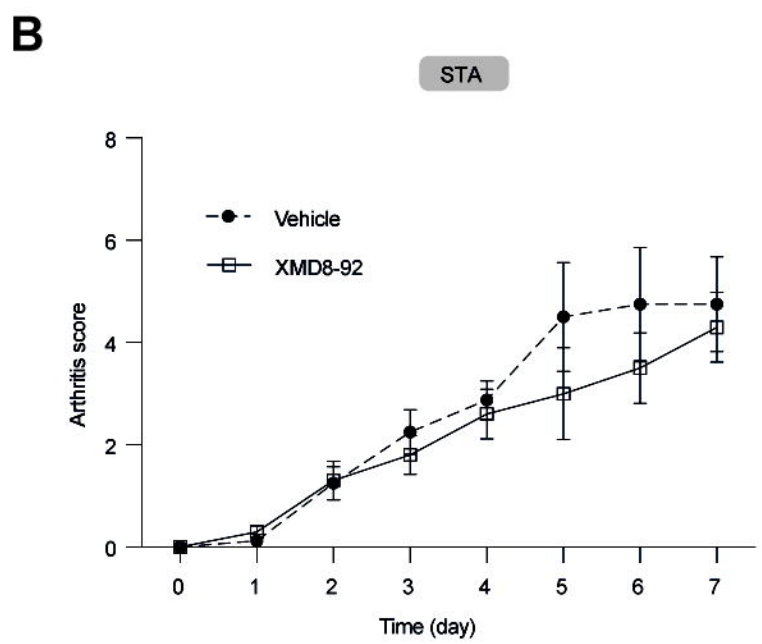
B
STA
Vehicle
XMD8-92
Arthritis score
Time (day)
0
2
4
6
8
0
1
2
3
4
5
6
7

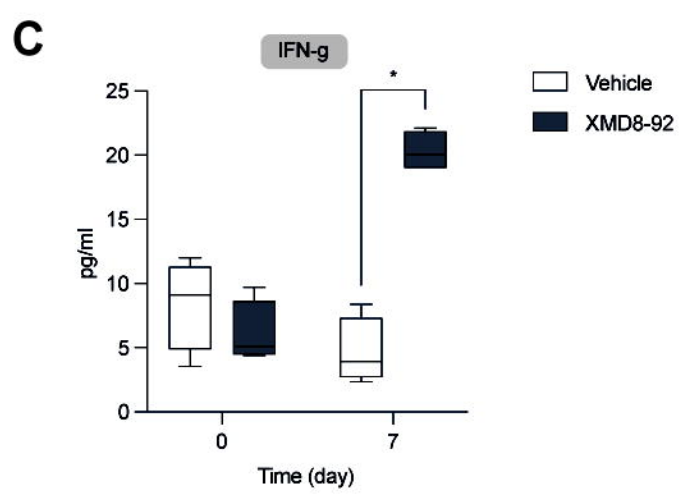
C
IFN-g
Vehicle
XMD8-92
pg/ml
Time (day)
0
5
10
15
20
25
0
7
*

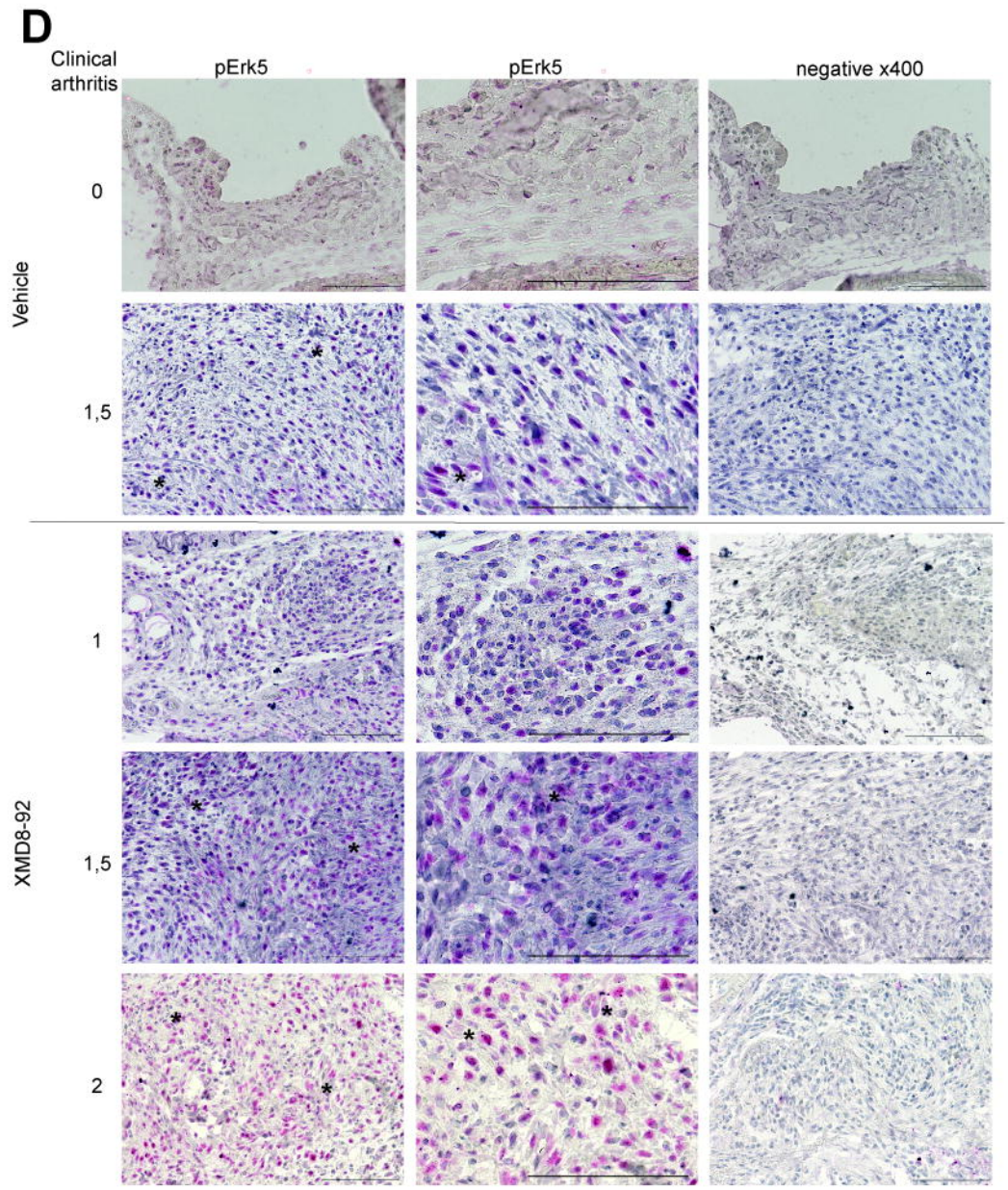
D
Clinical arthritis
pEr5
pEr5
negative x400
Vehicle
0
1,5
XMD8-92
1
1,5
2

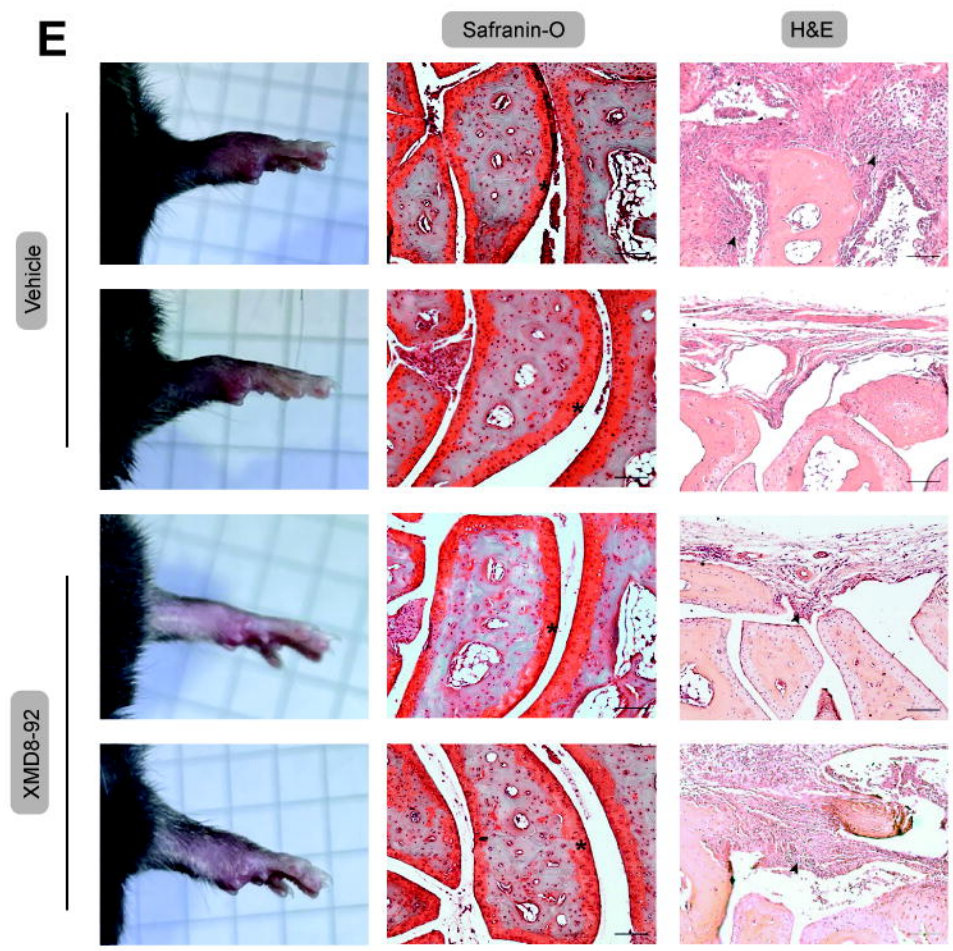
E
Safranin-O
H&E
Vehicle
XMD8-92

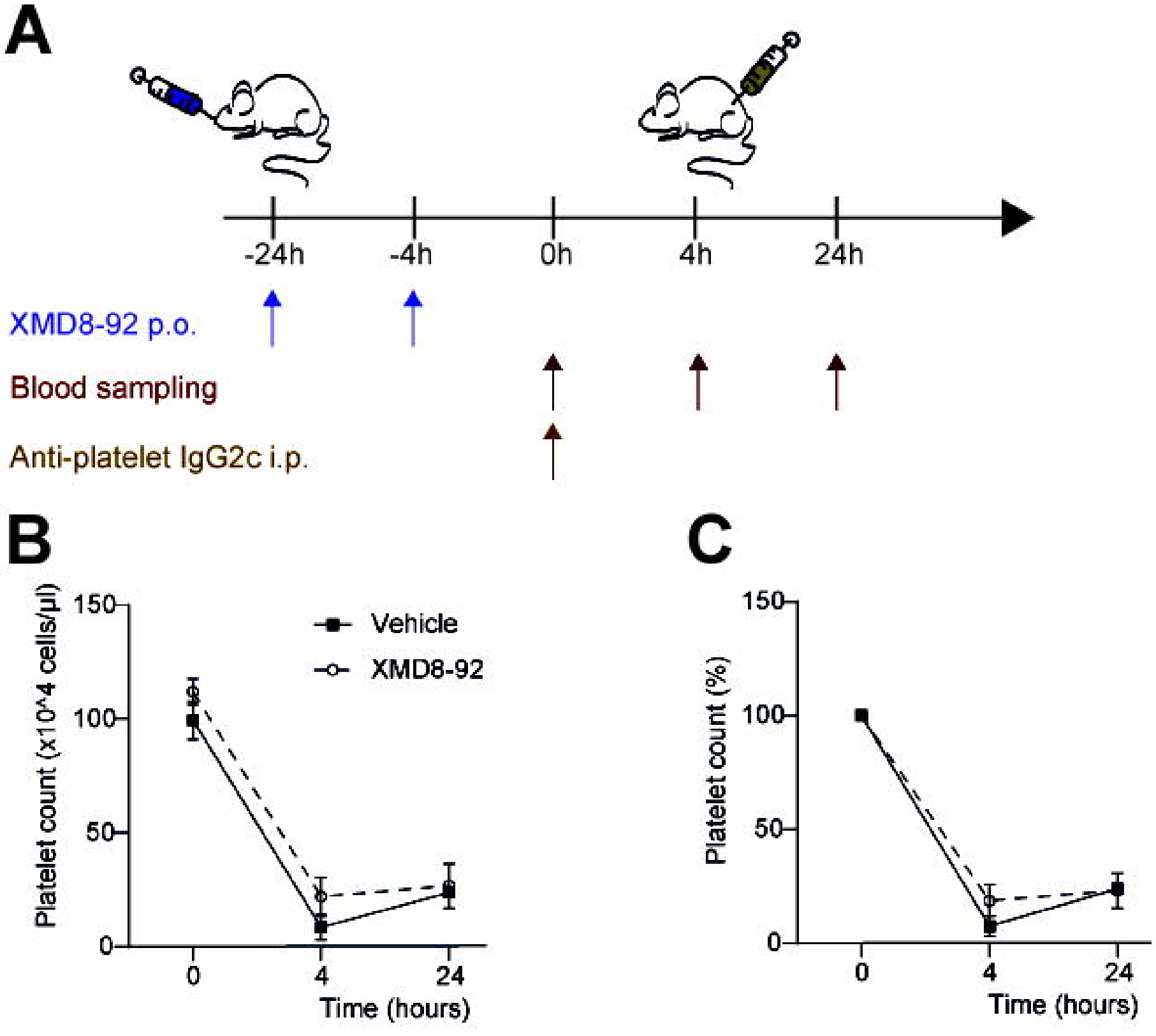
A
-24h
-4h
0h
4h
24h
XMD8-92 p.o.
Blood sampling
Anti-platelet IgG2c i.p.
B
Platelet count (x10^4 cells/µl)
150
100
50
0
Vehicle
XMD8-92
0
4
24
Time (hours)
C
Platelet count (%)
150
100
50
0
0
4
24
Time (hours)